Arab J Sci Eng (2017) 42:2021–2030
DOI 10.1007/s13369-017-2434-1

RESEARCH ARTICLE - MECHANICAL ENGINEERING

Effects of Process Parameters on Hot Extrusion of Hollow Tube

Jabbar Gattmah[1,2] · **Fahrettin Ozturk**[3] · **Sadettin Orhan**[1]

Received: 28 June 2016 / Accepted: 19 January 2017 / Published online: 8 February 2017

Abstract The control of hot extrusion process is a highly complicated task due to high deformation and high billet temperature during the process. A high-quality product can be produced by controlling the process temperature. In this present study, hot extrusion process of hollow tube is modeled by finite element method. Effects of process parameters, initial billet temperature, ram displacements, reduction of area, semi-die angle, and friction coefficients are studied. Finite element results are compared with the experimental results from previous studies. The results reveal that there is a good agreement between simulations and experiments. It is determined that reduction of area and friction coefficient have strong effects on surface temperature and extrusion force. The surface temperature is increased with increasing ram displacement and decreased gradually at the exit of the die due to heat transfer with the environment. Extrusion forces are increased up to friction coefficient of 0.35 for 13 and 25% reduction of areas. However, extrusion forces are not changed significantly after 0.2 coefficient of friction for 37 and 48% reduction of areas.

Keywords Finite element modeling · Hollow tube extrusion · Hot extrusion modeling · Surface temperature · Extrusion force

✉ Fahrettin Ozturk
fahrettin71@gmail.com

[1] Department of Mechanical Engineering, Ankara Yildirim Beyazit University, Ankara, Turkey

[2] Department of Mechanical Engineering, Diyala University, Diyala, Iraq

[3] Department of Mechanical Engineering, The Petroleum Institute, Abu Dhabi, UAE

1 Introduction

Hot extrusion process is one of the metals forming processes to produce several types of profiles, which are widely used in many manufacturing industries. Modeling of the hot extrusion process is a very complex job due to the combined effects of temperature fields and process parameters. The process generates very large deformations and high temperatures. Several process parameters, billet temperature, reduction of area, die semi-angle, ram speed, and extrusion pressure, which are interrelated with each other, affect the process. Therefore, the simulations of tube extrusion process are extremely difficult [1]. The optimal choice of the parameters can result in a good end product. Among these parameters, the most important parameter is the extrusion temperature since the initial billet temperature is different from the actual extrusion temperature during the cycle process [2]. It is reported that temperature variation depends on initial billet temperature, flow stress vs. strain at specific temperature and strain rate, plastic deformation, friction, and heat conduction between billet with die and mandrel as well as heat convection between ambient surrounding with die and mandrel [3]. Comparison between square and round dies to produce aluminum products has been studied by Chanda et al. [4] using a 3D finite element model. The study showed that the stress at the surface of the round extrusion is much lower than at the corner of the square extrusion. Hansson and Jansson [5] used two different regression models: a linear polynomial model and another model with interaction terms to investigate the analysis of hot tube extrusion of a glass-lubricated stainless steel by applying the finite element method in order to determine a link between the extrusion force and the initial billet temperature. Predictions of the regression models were quite successful. The results indicate that the extrusion force strongly depends on the initial billet

temperature. Hansson [6] simulated a glass-lubricated stainless steel tube extrusion in 2D and 3D considering a radial symmetry using MSC Marc software. The accuracy of an axisymmetric extrusion simulation was improved by Altan et al. [7] to determine temperature distribution. The results of temperature estimation using the axisymmetric extrusion showed a good agreement and reasonable accuracy. There have been several techniques to measure the temperature on the bearing surface. Terčelj et al. [8] developed a split die to improve the measurement accuracy of temperature for hot extrusion of aluminum. The study showed that local cooling where is near to bearing surface should be done because of possibility to remove the heat which is generated as a result of friction between the extruded profile and the die bearing surface. Parkar [9] studied process parameters of extrusion ratio or reduction of area, billet temperature, and ram velocity experimentally and numerically using conical and flat dies. The numerical model showed that the constant temperature and the strain rate can be achieved by making proper changes in material properties. Zhao et al. [10] studied the effect of the deformation speed on the microstructure and mechanical properties for AA6063 experimentally and numerically. The result reveals that the variations in extrusion wheel velocity heavily influence the maximum extrusion temperature. Mahmoodkhani et al. [11] predicted pressure and temperature histories of hot extrusion process successfully for AA3003. Kim et al. [12] conducted a coupled finite element analysis with an optimization technique for an optimal die design by controlling strain rate of workpiece during hot extrusion. Extrusion die profiles were defined by Bezier curves. Flexible polyhedron search (FPS) method was used as an optimization technique. Goodarzi and Serajzadeh [13] developed a thermo-mechanical model of hot extrusion processes. In their research, extrusion pressure and temperature variations within the metal and the die under both isothermal and non-isothermal conditions were studied to estimate force-displacement diagrams by both of upper bound and Petrov–Galerkin finite element analysis according to the velocity field for AA6061-10%SiC_p. The results were in reasonable agreement. The effect of the ram speed and ram displacement on the exit temperature by a finite element simulation of isothermal extrusion for 7075 aluminum alloy was investigated by Yang et al. [14] to produce a large-size tube with a piece-wing. The results for isothermal extrusion showed that the ram displacement increases with decreasing the ram speed and the exit temperature increases for the large-size tubes with the piece-wing. Bressan et al. [15] modeled a metal extrusion by flow formulation. Governing equations were discretized by finite volume method using Explicit MacCormack method in structured and collocated mesh. The study proved that that MacCormack and SIMPLE methods can be applied in the solution of metal forming processes. In another study, hot extrusion was used to fabricate a magnesium matrix composite reinforced with 5 wt% AIN particles to show the effect of the hot extrusion on microstructure and mechanical properties [16]. It was concluded that the matrix grain was significantly refined after the hot extrusion. Rahim et al. [17] investigated the influences of ram speed, preheat temperature, and preheat time on the responses flow stress and heat distribution. The results showed that the temperature 500 °C on the cross section becomes more inhomogeneous at the higher ram speed. Numerous studies have indicated that the temperature field during hot extrusion is very complicated. However, they have neglected the effect of the tools profiles on thermal and mechanical responses when the high temperature is generated at forming zone. A few researchers have studied the effect of velocity, ram displacement, and extrusion ratio on extrusion force without considering thermal parameters. For example, Refs. [5,6] did not take into consideration the effects of geometrical parameters (semi-die angle and reduction of area) on extrusion force and surface temperature. Hansson and Jansson [5] performed a study on temperature field without considering geometric parameters. It is necessary to consider the combined effects of dies and mandrels with the initial billet temperature and the coefficients of friction. Therefore, there is a great need to link between reduction of area, friction coefficient, semi-die angle, and initial billet temperature with ram displacement to study temperature behavior and extrusion force during the hot extrusion process in order to understand the process deeply. In this study, an axisymmetric finite element model for the hot extrusion process was developed by using a commercially available software ABAQUS 6.14-2 to determine the effects of initial billet temperature (T_i), ram displacement, reduction of area ($R\%$), semi-die angle (α), friction coefficient (m) on both of surface temperature and extrusion force. The *dynamic/temp-disp/explicit* analysis has been applied to estimate the states of stresses and temperature distributions during the extrusion process for stainless steel AISI 316L to produce large-size hollow tubes. The accurate modeling is quite important in order to get cheap, accurate product in a short period of time.

2 Direct or Forward Hot Extrusion Process for Hollow Tube

In this study, the direct hot extrusion method was used. Schematic representation of the process is shown in Fig. 1. In the process, the billet is heated to the required temperature first, and then it is extruded along the same direction of the ram or punch. Frictions between die and billet and mandrel and billet are quite important. In the hot extrusion process, several factors affect temperature variation: flow stress versus strain based on temperature and strain rate, plastic deformation (homogenous and redundant work), friction coefficient

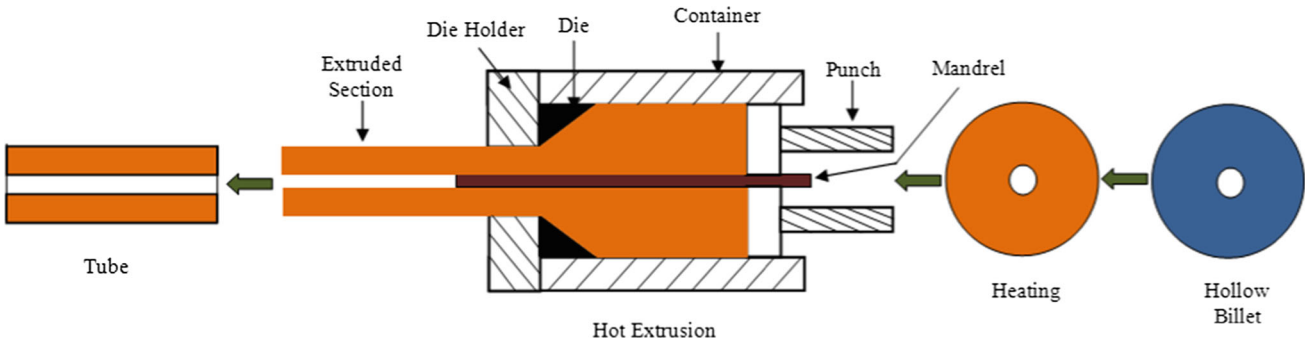

Fig. 1 Direct hot extrusion process for a hollow tube

Table 1 Chemical composition of AISI 316L [20]

C	Si	Mn	P	S	Cr	Mo	N	Ni
≤0.020	≤1.00	≤2.00	≤0.045	≤0.015	16.50–18.50	2–2.5	≤0.11	10–13

Table 2 Mechanical and thermal properties of AISI 316L [20]

AISI 316L	Young's modulus	195 GPa	Ultimate tensile stress	550 MPa
	Density	7.97 g/cm^3	Thermal expansion	16.5 × 10^{-6}/K
	Poisson's ratio	0.27	Thermal conductivity	15 W/mK
	Yield strength	290 MPa	Specific heat	0.5 J/g °C

between billet and die and mandrel, and heat transfer between tool and billet and ambient surrounding [18].

3 Mechanical Properties and Experimental Data of Flow Stress–Strain

The billet material was AISI316L stainless steel, and the chemical composition of the material is given in Table 1. Both materials of the die and the mandrel were AISI H13 stainless steel. Table 2 displays mechanical and thermal properties of AISI 316L. Flow stress is predominantly related thermo-mechanical parameters: strain, strain rate, and temperature [19]. In this study, the compression flow curves for strain rates of 0.01, 1, and 10 s^{-1}with four temperatures of 200, 400, 800, and 1100 °C were considered. Figure 2 shows flow curves for various temperatures at a strain rate of 0.01 s^{-1}. It is quite obvious that true stress reduces significantly with increasing temperature. At the temperature of 1100 °C, flow curve of the materials looks like a perfectly plastic material. A constant stress with increasing temperature was observed.

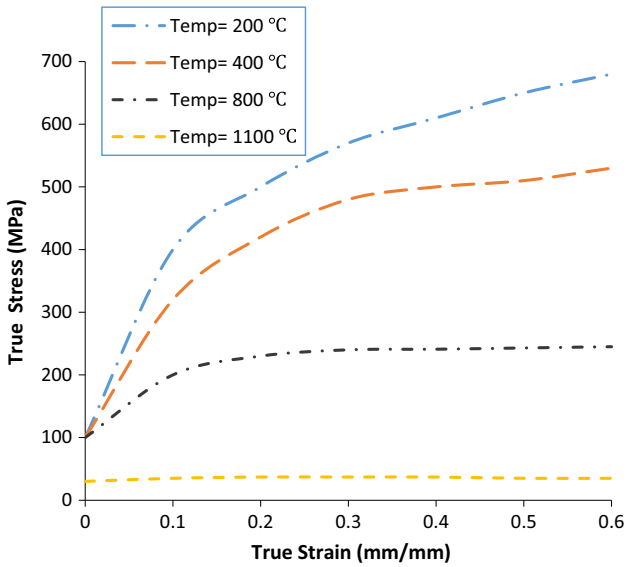

Fig. 2 Flow curves for various temperatures at the strain rate of 0.01 s^{-1} [6]

4 Finite Element Modeling for Hot Extrusion of Hollow Tube

In the tube hot extrusion process, the problem is a thermo-mechanical due to pressure-dependent thermal contact resistance between billet with die and mandrel. Thermal coupling takes places because of either large deformation or contact. Inelastic deformation generates heat which causes thermal coupling due to an increase in billet entropy. Coupled thermo-mechanical analysis procedures are presented as a flow chart in Fig. 3 [21]. Mechanical and thermal properties which were used in the analysis are summarized in Table 2. Heat transfers between billet, tooling, and ambient surrounding medium are expressed as described in Eq. 1. A material model is coupled

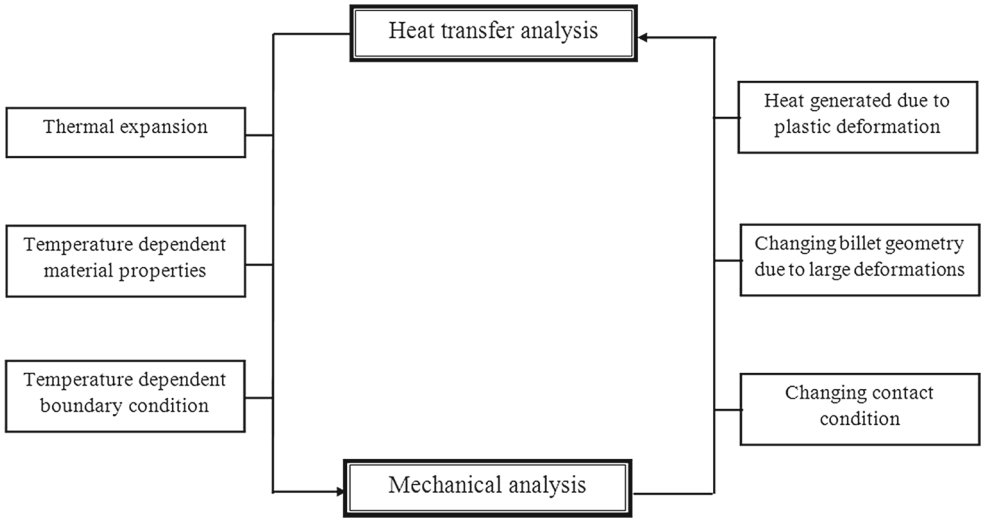

Fig. 3 Coupled thermo-mechanical analysis [21]

with a heat transfer model [14].

$$(KT_{yi})_{yi} + \dot{r} - (\rho c_p T) = 0 \tag{1}$$

The term $(KT_{yi})_{yi}$ represents the heat transfer rate where K is the thermal conductivity and T the temperature, while the term $\left(\rho c_p T\right)$ is the internal heat generation rate. Where ρ is the specific density and c_p is the specific heat as well as $\dot{r}$ denotes the heat generation rate. Plastic deformation leads to the rate of the heat generation in extrusion that can be calculated by Eq. 2.

$$\dot{r} = \alpha\rho \tag{2}$$

In equation, α is the fraction of mechanical energy and is mostly taken as a 0.9. The heat flux is given along the boundary of model. By using the weighted residual method, the energy balance equation can be written in Eq. 3 as following:

$$\int_v KT_{yi}\partial T_{yi}\,\mathrm{d}V + \int_v \alpha c_p \dot{T}\partial T\,\mathrm{d}V - \int_v \alpha\bar{\sigma}\bar{\varepsilon}\,\partial T\,\mathrm{d}V - \int_s q_n\,\partial T\,\mathrm{d}S = 0 \tag{3}$$

The q_n is the heat flux normal to the boundary surface that contains heat loss as results of the heat convection and radiation to environment between billet and die with mandrel as well as the heat loss during contact with other hotter or colder objects. The temperature distributions of billet, die, and mandrel can be found easily by using Eq. 3. Accurate simulation results can be obtained with a good constitutive model depends on the physical parameters. The material is assumed to be an elastic-plastic that is used extensively for the steady-state forming condition. The velocity field with respect to the material formulation is determined by minimizing the functional equation as described.

$$\delta\emptyset = \int_v \bar{\sigma}\delta\dot{\bar{\varepsilon}}\,\mathrm{d}V + \int_v k\,\dot{\varepsilon}_{kk}\delta\dot{\varepsilon}_{mm}\,\mathrm{d}V + \int_v \bar{F}_i\delta_{vi}\,\mathrm{d}S = 0 \tag{4}$$

where $\bar{\sigma}$ is effective stress, $\dot{\bar{\varepsilon}}$ represents effective strain rate, $\dot{\varepsilon}_{kk}$ is known strain rate, and vi is velocity component. V is the volume of the billet, $\bar{F}_i$ is known the traction (frictional) stress and k a large positive constant to penalize volume change (commonly known as Lagrange Multiplier). Three types of nonlinearities are occurred. These are material, geometric, and nonlinear boundary condition. The material nonlinearity is related with the relationship between stresses and strains based on the strain rate and temperature. A nonlinear solution for hot extrusion of hollow tube is obtained by Newton–Raphson method. In steel extrusion simulation, strain rates are higher than what is normally used in tests. This fact causes the difference between results. For the AISI 316L stainless steel, material model is defined with a dislocation density. However, in finite element simulation, compression test data at different temperatures and strain rates (Fig. 2) were used. Obviously, it is different than the material model with a dislocation density. In the isotropic rigid plastic model, flow stress is functions of effective strain, effective strain rate, and temperature as described in Eq. 5.

$$\bar{\sigma} = \bar{\sigma}\left(\bar{\varepsilon}, \dot{\bar{\varepsilon}}, T\right) \tag{5}$$

The geometric nonlinearities in the hot extrusion are given by the existence of large strains and deformations. In this study, large displacement-large strain is based on the analysis of

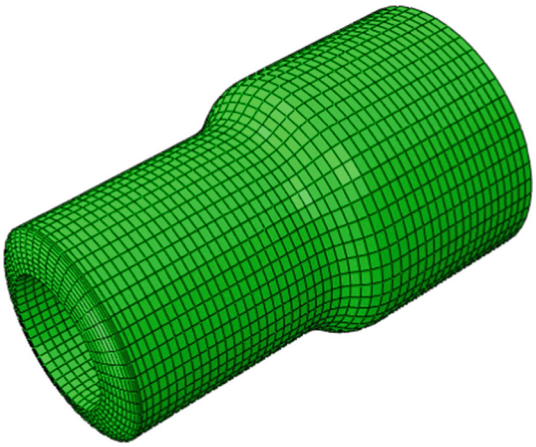

Fig. 4 Deformed meshed of the hot extrusion for hollow tube

the geometric nonlinearities, and kinematic of deformation is described by Arbitrary Eulerian–Lagrangian. Arbitrary Lagrangian Eulerian ALE meshing combines the features of pure Lagrangian analysis and pure Eulerian analysis. So, it is used with *explicit, temp, displacement, dynamic* that allows to maintain a high-quality mesh throughout dynamic analysis and makes the mesh move independently of the material when occurring large deformation or losses of material with the mesh topology remains unchanged. The mesh and the quadrature points move according to the material and deform with material flow when the constitutive equations are determined at the some point during the whole analysis as shown in Fig. 4. In the ABAQUS software, a four thermally coupled axisymmetric quadrilateral, bilinear displacement and temperature, reduced integration, hourglass control element CAX4RT was chosen. The billet was modeled as an axisymmetric with 500 elements. The boundary conditions are displayed in Fig. 5. Boundary nonlinearity in the hot extrusion of hollow tube represents contact between deformable (workpiece) to the rigid body contact (die) and the deformable (workpiece) to the rigid body contact (mandrel). The frictional constraints were defined in the interaction condition. In the procedure of explicit/temp/dis/dynamic, surface-to-surface (explicit) was developed to create an interaction. Finite sliding with a penalty contact method was applied for all contacts to resolve tangential behavior of a mechanical contact. In this method, the compressive force is proportional to the penetration of the material, using the basic concept of the Coulomb friction model. Contact interaction property was selected to define heat generation, normal behavior (hard contact), and tangential behavior with different friction coefficients as presented in Table 3. The surface and contact heat transfer coefficients were taken to be (0.66 kW/m^2/°C) and (9 kW/m^2/°C), respectively [6]. The frictional shear stress can be obtained by Eq. 6 as given.

$$\tau_f = m\left(\frac{\bar{\sigma}}{\sqrt{3}}\right) \tag{6}$$

In Eq. 6, $\bar{\sigma}$ is the effective flow stress of the deformed material, and m is friction coefficient. Die and mandrel were fixed with all directions and a velocity of 0.042 m/s was applied on ram at the extrusion direction as illustrated in Fig. 5. The die and mandrel were defined as rigid bodies and fixed at all directions. The initial temperatures of them are 20 and 100 °C, respectively, for all simulations at various initial billet temperatures. In this work, the maximum of semi-die angle of 45° was selected since there will be a dead zone if it is greater than this value [22]. In addition, the fillets of the die at the inlet and the outlet were selected based on the die length. Table 3 shows all initial parameters and dimensions that were used for the simulations.

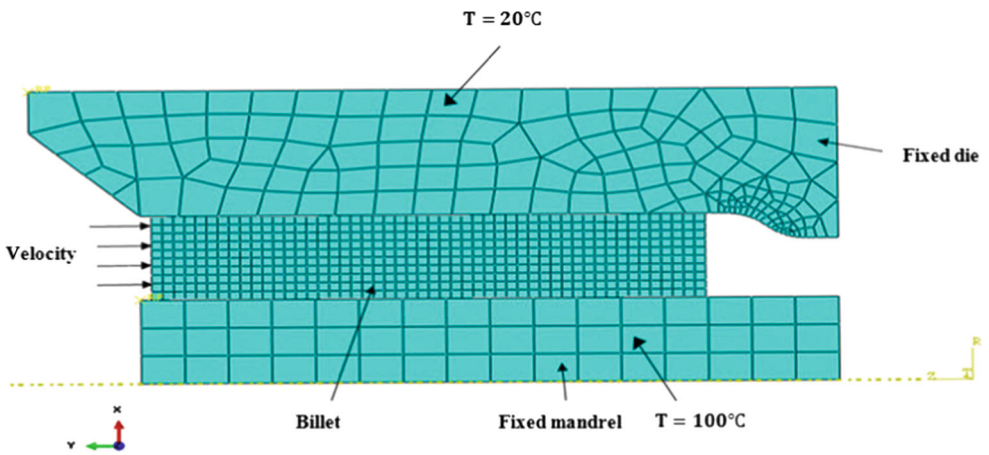

Fig. 5 Axisymmetric finite element boundary conditions of the hollow tube hot extrusion process

Table 3 Parameters and dimensions of hollow tube hot extrusion model for finite element simulations

Outer diameter of initial billet (cm)	Diameter of mandrel (cm)	Length of initial billet (cm)	Initial thickness of billet (cm)	Initial billet temp. T_i (°C)	Thickness of final tube (cm)	Reduction of area ($R\%$)	Die semi-angle (α) (°)	Friction coefficient (m)
40	10	50	10	800	9	13	15	0.05
							20	0.10
							25	0.15
				900	8	25	30	0.20
							35	0.25
							40	0.30
				1000	7	37	45	0.35
								0.40
				1100	6	48		

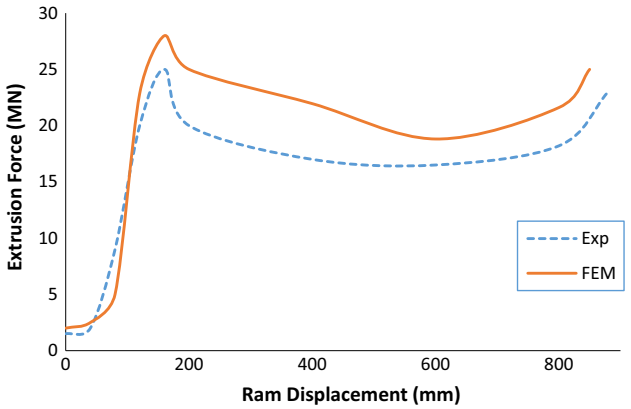

Fig. 6 Comparison of extrusion force versus ram displacement between experimental [5] and finite element

5 Results and Discussion

5.1 Model Validation

The experimental results were obtained from a previous study by Hansson and Jansson [5]. Figure 6 shows the relationship between the ram displacement and the extrusion force for both the experimental and the finite element. In the experimental work of Hansson and Jansson [5], the initial dimensions of billet were 240 mm × 112 mm × 888 mm (Outer diameter × inner diameter × length). The initial billet temperature was 1150 °C and the die and the mandrel temperatures were 300 °C. The final tube diameter was 142 mm with a 22 mm thickness. Coulomb friction coefficient of 0.023 was used for glass-lubrication on contact areas, and a contact heat transfer coefficient 1500 $\mathrm{W}/\left(\mathrm{m}^2\mathrm{K}\right)$ was assumed. The results show a good agreement between the experimental and the finite element as shown in Fig. 6. This good correlation indicates that the boundary conditions and initial conditions of the model were proposed in this study were sufficiently accurate. Extrusion force reached the maximum value when ram displacement was about 160 mm. Figure 6 illustrates that both of the curves have same trend. However, the required force for the experiment is lower than the finite element due to higher yield stress and strain hardening inputted to the software [23]. According to the pervious study by Hansson [6], the initial dimensions of billet were 121 mm × 33 mm × 421 mm and the ram speed was 93 mm/s. The final tube diameter became 33.2 with a tube thickness 3.5 mm. The initial temperatures for initial billet, mandrel, and die are 1100, 200, and 20 °C in order. In the simulation, the friction coefficient was taken as 0.03. Figure 7 displays comparison of the experimental and finite element results for exit temperature vs. time on surface during the extrusion process [6]. The exit surface temperature was experimentally recorded with an extruded length of 27.9 mm at the beginning of extrusion on the outer surface of the final tube. In the finite element analysis, a 425 mm extrude of tube was simulated. The results of exit temperature on the surface reveal a substantial convergence with little difference at the beginning of the extrusion. The large disparity was at 0.1 s when the exit temperature difference was 35 °C between the experimental and the finite element. The difference reaches 25 °C at 0.15 s. Two main factors may cause these differences. The first one could be the sensitivity of the optical pyrometer during the measurement. The second one may be the assumption of initial billet temperature which is constant in the finite element; however, it is a fact that the billet has temperature gradients [6]. After verification of the model, effects of initial billet temperature, ram displacement, reduction of area, semi-die angle, and friction coefficient on surface temperature and extrusion force were thoroughly studied.

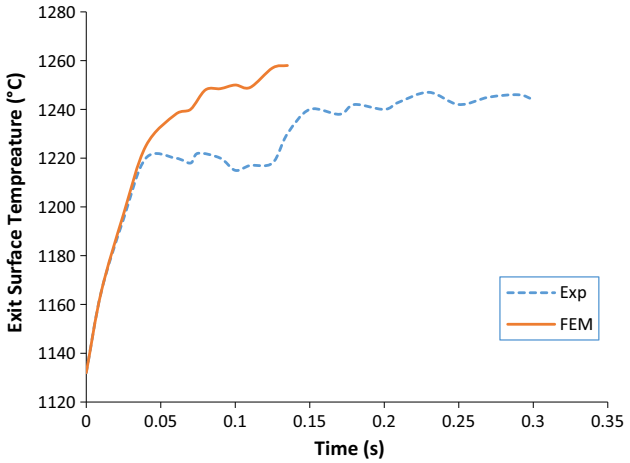

Fig. 7 Comparison between experimental [6] and finite element results for exit surface temperature versus time

5.2 Thermal Stress Distribution in the Deformed Billet

Effects of initial billet temperatures on flow stress were shown in Fig. 8. The figure displays the effects of flow stress at both low and high initial billet temperature 800 and 1100 °C, respectively. For the low initial temperature of 800 °C, the flow stress was higher than initial billet temperature of 1100 °C (Fig. 6b). It is a well-known fact that the flow stress increases with decreasing of temperature. Material gets softer at high temperatures. That is, the rising in initial billet temperature makes flow in forming zone easier [24], and then the flow stress has been decreased and plasticity increased due to the increase in diffusion of solute atoms. The flow stress is also decreased with increasing strain rate [6]. In Fig. 8a, b, it can be seen that thermal stress in forming zone at near the mandrel less than at near the die because the initial temperature of mandrel (100 °C) is more than initial temperature of die temperature of 20 °C.

5.3 Temperature Distribution in the Deformed Billet with Different Ram Displacements

Effect ram displacement on temperature distribution of the deforming billet is summarized in Fig. 9a–c. The figures show the temperature distribution on the billet for ram displacements of 180, 247, and 420 mm, respectively. It is clearly seen that the temperature is higher at contact slope surface and decreases gradually until reaches near the billet center. Figure 9a shows when the billet moves to the deformation zone, it starts rising with increasing friction between the billet and the die and the billet and the mandrel. Because of the severe shear, the maximum temperature appears at the junction of the die bearing and the face of die [2]. The temperatures of the billet near the die face always increase at along the die bearing surface during the subsequent steady-state extrusion. The temperature of the intermediate layer is higher, and it continues increasing as displayed in Fig. 9b. The temperature was recorded as 950 °C at the exit of deformation zone as seen in Fig. 9c. In Fig. 9c, the temperature decreases gradually at the exit due to heat transfer between the tube and the surrounding environment. As a result, the temperature was increased with increasing ram displacement through the extrusion process. It is known that more reduction of areas mean large deformation and more internal work. It is an indication of internal heat which is seen as a temperature increase.

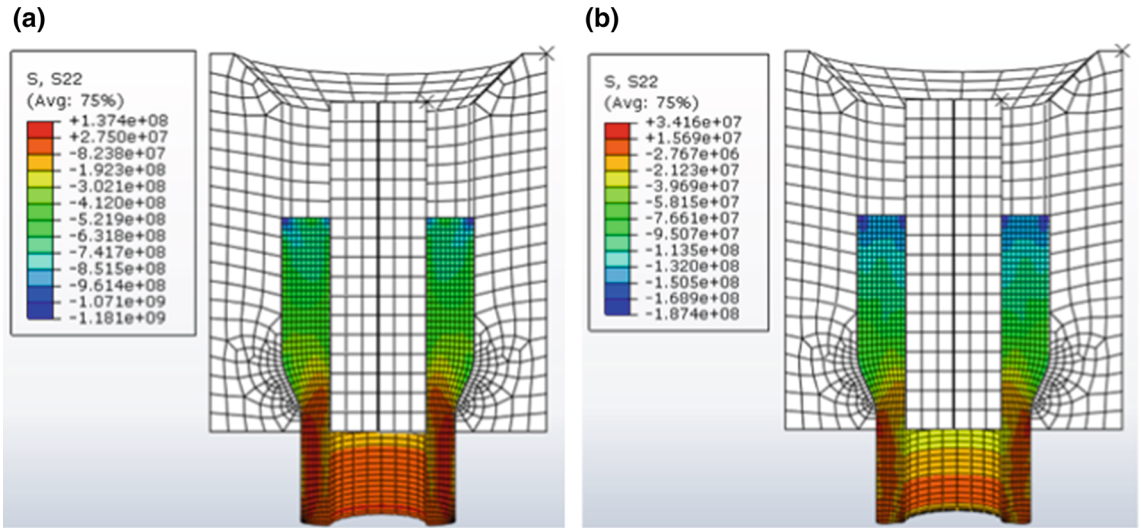

Fig. 8 Flow stress distribution **a** initial billet temperature of 800 °C and **b** initial billet temperature of 1100 °C($\alpha = 25°$, $R = 48\%$, $m = 0.15$, extrusion velocity of 0.042 m/s and ram displacement of 231 mm)

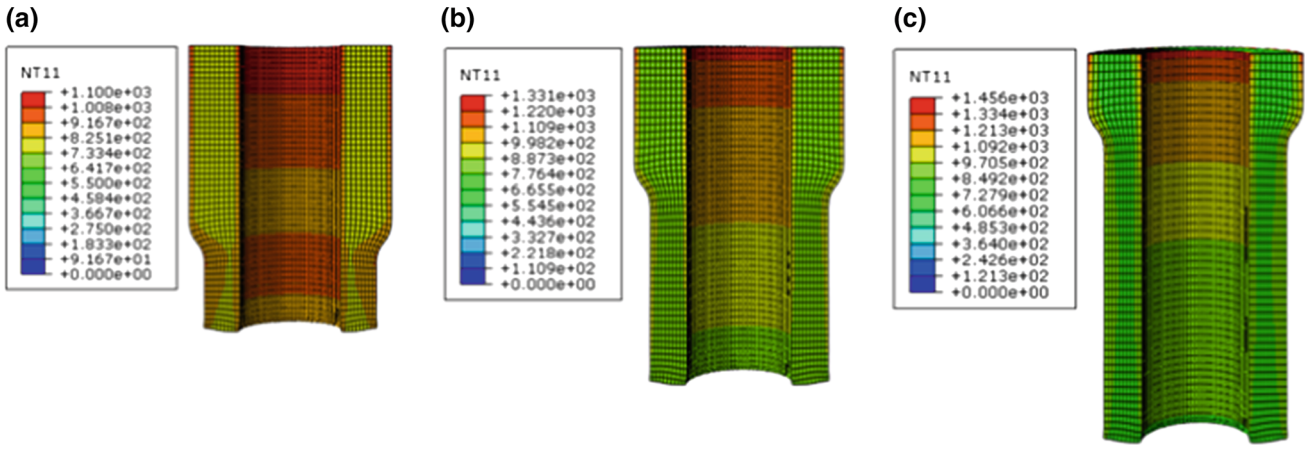

Fig. 9 Temperature distribution versus ram displacement **a** 180 mm, **b** 247 mm, and **c** 420 mm ($T_i = 800\,^{\circ}\text{C}$, $\alpha = 40^{\circ}$, $m = 0.15$, and $R = 37\%$)

5.4 Ram Displacement Versus Surface Temperature at Various Reduction of Areas

Figure 10 indicates the relationship between ram displacements versus surface temperatures during extrusion process for various reduction areas with initial billet temperature of 800 °C. There is appreciable clearance between ram and billet at the starting of ram movement; therefore, the only contact of the billet with the tools is at die face where the boundary conditions including friction has no direct effect on the deformation [25]. The temperature of the surface at forming zone increases with increasing of ram displacement. But the value is low due to the heat transfer between the tooling and the surrounding environment. The time for heat transfer is relatively short. It can also be seen that the temperature increases with increasing the reduction of area increases the relative energy consumption from plastic deformation. When the reduction of area R is 48%, the temperature was increased to 1010 °C. It was 845 °C when reduction of area was 13%. The reduction of area strongly affects surface temperature because of increasing plastic deformation at the inlet and the outlet of the forming zone.

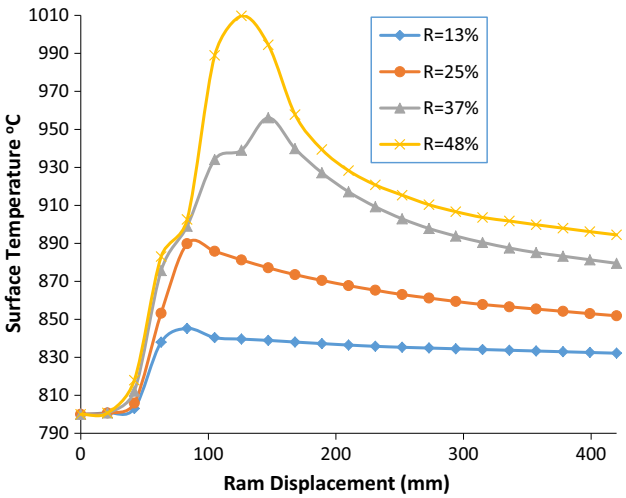

Fig. 10 Relationship between ram displacement versus surface temperature for various reduction of areas ($T_i = 800\,^{\circ}\text{C}$, $\alpha = 25^{\circ}$, $m = 0.2$, and extrusion velocity of 0.042 m/s)

5.5 Ram Displacement Versus Surface Temperature at Various Friction Coefficients

The effect of ram displacement on surface temperature for various friction coefficients was evaluated as is indicated in Fig. 11. It is clearly seen that the surface temperature increases with an increase in friction coefficient. Increased temperatures reduce the flow stress substantially. The maximum surface temperature reached 936 °C for a ram displacement of 84 mm and friction coefficient of 0.2. When friction coefficient of 0.05 and again a ram displacement of 84 mm was used, the surface temperature was decreased to 871 °C. These results indicate that the increase in friction causes a decrease in flow stress that is a function of temperature differential between initial and actual temperature that lead to increasing in overall temperature of the billet [25]. The increase in friction coefficient with the increase in ram displacement leads to an increase in heat due to the increase in plastic deformation in forming zone. Eventually, the exit surface temperature will increase. After material exit from the bearing die, the exit surface temperature starts to decrease due to heat transfer between the billet and ambient surrounding.

5.6 Die Semi-Angle Versus Extrusion Force at Various Initial Temperatures

Effect of semi-die angle on extrusion force for various initial temperatures was also studied. Results were summarized

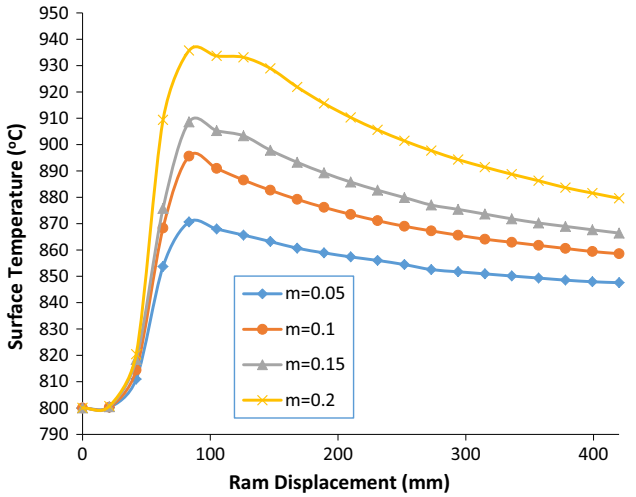

Fig. 11 Relationship between ram displacement and surface temperature for various friction coefficients ($T_i = 800\,°C$, $\alpha = 40°$, $R = 37\%$, extrusion velocity of 0.042 m/s)

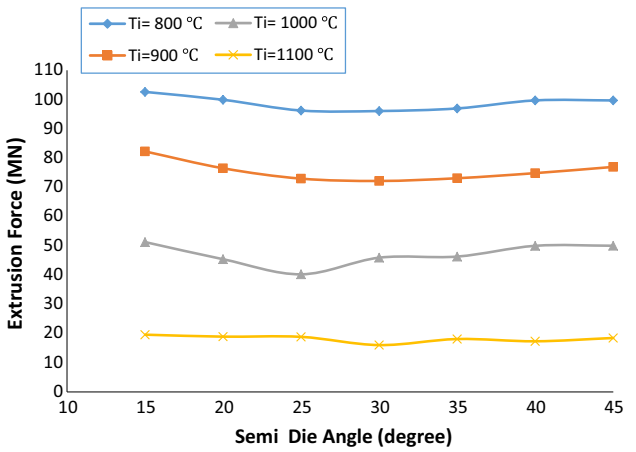

Fig. 12 Relationship between die semi-angle and extrusion force for various initial temperatures ($R = 48\%$, $m = 0.15$, and extrusion velocity of 0.042 m/s)

in Fig. 12, which reveals that the die semi-angles between 25° and 30° give the minimum extrusion force for all initial billet temperatures. General trend looks like a steady line. It means that semi-die angle does not have a significant effect on the extrusion force. The extrusion force decreases with increasing initial billet temperature, and the required force to extrude the metal in contact area is increased because the contact pressure increases. At the lower temperature, the flow stress increases that lead to the surfaces in contact produce a greater elastic deformation [25]. This is an expected result. It is a well-known phenomenon that flow stress is decreased with increasing temperature. The combination of low flow stress and fluidity of the billet help overcome the friction between die and billet.

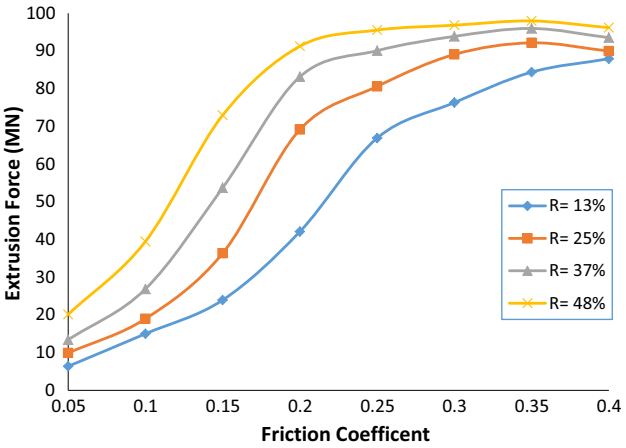

Fig. 13 Relationship between friction coefficient and extrusion force at various reduction of areas ($T_i = 900\,°C$, $\alpha = 25°$, and extrusion velocity of 0.042 m/s)

5.7 Friction Coefficient Versus Extrusion Force at Various Reduction of Areas

The effect friction coefficient on extrusion force for various reductions of areas is drawn as in Fig. 13. It is clear that extrusion force increase with increasing both friction coefficient and reduction of area. When the value of friction coefficient is between $m = 0.05-0.2$ extrusion force substantially increased for 13 and 25% reduction of areas. However, extrusion forces are not changed significantly after 0.2 coefficient of friction for 37 and 48% reduction of areas. The material flow depend on the friction force that restricts the movement of billet at extrusion direction. General trend is that the extrusion force is increased up to friction coefficient of 0.35. Because of the increasing of billet temperature leads to the decreasing of flow stress. All these results reveal that both reduction of area and friction coefficient affects the extrusion force considerably. The combined effect of friction coefficient and reduction of area causes an increase in billet temperature. The optimal choice of reduction of area and friction coefficient with initial billet temperature can be given a good quality product with less effort.

6 Conclusion

In this study, the finite element model of the hot extrusion process of a hollow tube was modeled, and the effects of process parameters were investigated. Following conclusions were drawn:

1. Proposed finite element model was verified with experimental results from literatures. Results were in good agreement. The proposed finite element model was quite

successful to study the hot extrusion process of a hollow tube.

2. The surface temperature is increased with increasing ram displacement, friction coefficient, and reduction of area and decreased gradually at the exit of the die due to heat transfer with the surrounding environment.
3. Die semi-angles between 25° and 30° give the minimum extrusion force for initial billet temperatures of 800, 900, 1000, and 1100 °C.
4. Extrusion forces are increased up to friction coefficient of 0.35 for 13 and 25% reduction of areas. However, extrusion forces are not changed significantly after 0.2 coefficient of friction for 37 and 48% reduction of areas. It means that higher friction coefficient is not quite effective at the higher reduction of areas.

References

1. Sheu, J.J.; Liang, J.M.: Hot extrusion die design and process simulation of unsymmetric structure. MSC Software. Simufact Technical Presentations. http://simcompanion.co.mscsoftware.mscsoftware.jp/sites/default/files/2013.3_Hot_extrusion_die_design_and_process_simulation_of_an_unsymmetrical_structure.pdf (2013)
2. Liu, G.; Zhou, J.; Duszczyk, J.: Finite element simulation of magnesium extrusion to manufacture a cross-shaped profile. J. Manuf. Sci. Eng. **29**, 607–614 (2007)
3. Saha, P.K.: Aluminum Extrusion Technology. ASM International, Materials Park, Ohio (2000)
4. Chanda, T.; Zhou, J.; Duszczyk, J.: FEM analysis of aluminium extrusion through square and round dies. Mater. Des. **21**, 323–335 (2000)
5. Hansson, S.; Jansson, T.: Sensitivity analysis of a finite element model for the simulation of stainless steel tube extrusion. J. Mater. Process. Technol. **210**, 1386–1396 (2010)
6. Hansson S.: Simulation of stainless steel tube extrusion. Licentiate thesis, Luleå University of Technology, Swedish (2006)
7. Altan, B.; Geverk, M.; Onurlu, S.: A numerical method for predicting the tempreature distribution in axisymmetric extrusion through flat dies. J. Mech. Work. Technol. **13**, 151–162 (1986)
8. Terčelj, M.; Turk, R.; Kugler, G.; Fajfar, P.; Cvahte, P.: Measured temperatures on die bearing surface in aluminium hot extrusion. RMZ Mater. Geoenviron. **53**, 163–173 (2006)
9. Parkar, A.A.: On modeling and experimental validation of extrusion process of lightweight alloys. M.Sc thesis, Mississippi State University (2011)
10. Zhao, Y.; Song, B.; Pei, J.; Jia, C.; Li, B.; Linlin, G.: Effect of deformation speed on the microstructure and mechanical properties of AA6063 during continuous extrusion process. J. Mater. Process. Technol. **213**, 1855–1863 (2013)
11. Mahmoodkhani, Y.; Wells, M.A.; Parson, N.; Poole, W.: Numerical modelling of the material flow during extrusion of aluminium alloys and transverse weld formation. J. Mater. Process. Technol. **214**, 688–700 (2014)
12. Kim, N.; Kang, C.; Kim, B.: Die design optimization for axisymmetric hot extrusion of metal matrix composites. Int. J. Mech. Sci. **43**, 1507–1520 (2001)
13. Goodarzi Hosseinabadi, H.; Serajzadeh, S.: Hot extrusion process modeling using a coupled upper bound-finite element method. J. Manuf. Process. **16**, 233–240 (2014)
14. Yang, H.; Zhan, J.; He, Y.; Han, B.: Effect of temperature and ram speed on isothermal extrusion for large-size tube with piece-wing. J. Mater. Sci. Technol. **21**, 499–504 (2005)
15. Bressan, J.; Martins, M.; Button, T.: Analysis of aluminum hot extrusion by finite volum method. J. Mater. Today **2**, 4744–4747 (2015)
16. Chen, J.; Bao, J.; Chen, F.: Evolutions of microstructure and mechanical properties for Mg–Al/AIN composites under hot extrusion. Mater. Sci. Eng. A **667**, 426–434 (2016)
17. Rahim, S.; Lajis, M.; Ariffin, S.: Effect extrusion speed and tempreature on hot extrusion process of 6061 aluminum alloy chip. ARPN J. Eng. Appl. Sci. **11**, 2273-227 (2016)
18. Abecassis, J.; Abbou, R.; Chaurand, M.; Morel, M.; Vernoux, P.: Influence of extrusion conditions on extrusion speed, temperature, and pressure in the extruder and on pasta quality. Cereal Chem. **71**, 247–253 (1994)
19. Jonas, J.; Sellars, C.; Tegart ,W.: Strength and structure under hot-working conditions. J. Metall. Rev. **14**, 1–24 (1969)
20. Tolosa, I.; Garciandía, F.; Zubiri, F.; Zapirain, F.; Esnaola, A.: Study of mechanical properties of AISI 316 stainless steel processed by "selective laser melting", following different manufacturing strategies. Int. J. Adv. Manuf. Technol. **51**, 639–647 (2010)
21. Ana, S.: MSC Mark 2003 Introductory Course. MSC Software Corporation, Newport Beach (2003)
22. Qamar, S.: FEM study of extrusion complexity and dead metal zone. Arch. Mater. Sci. Eng. **36**, 110–117 (2009)
23. Onuh, S.; Ekoja, M.; Adeyemi, M.: Effects of die geometry and extrusion speed on the cold extrusion of aluminium and lead alloys. J. Mater. Process. Technol. **132**, 274–285 (2003)
24. McQueen, H.J.; Spigarelli, S.; Kassner, M.E.; Evangelista, E.: Hot Deformation and Processing of Aluminum Alloys. CRC Press, Boca Raton (2011)
25. Flitta, I.; Sheppard, T.: Nature of friction in extrusion process and its effect on material flow. Mater. Sci. Technol. **19**, 837–846 (2003)